Polish Society of Composite Materials
Polskie Towarzystwo Materiałów Kompozytowych

19: 2 (2019) 56-63

COMPOSITES THEORY AND PRACTICE
ISSN: 2084-6096
ISSN (online): 2299-128X

Wiesław Frącz[1]*, Grzegorz Janowski[2]

[1] *Rzeszow University of Technology, Faculty of Mechanics and Technology, Department of Integrated Design and Tribology Systems al. Kwiatkowskiego 4, 37-450 Stalowa Wola, Poland*
[2] *Rzeszow University of Technology, Faculty of Mechanical Engineering and Aeronautics, Department of Materials Forming and Processing al. Powstańców Warszawy 8, 35-959 Rzeszów, Poland*
**Corresponding author. E-mail: wf@prz.edu.pl*

Received (Otrzymano) 24.04.2019

PREDICTING EFFECT OF FIBER ORIENTATION ON CHOSEN STRENGTH PROPERTIES OF WOOD-POLYMER COMPOSITES

The paper presents an assessment of the effect of fiber orientation on the strength properties of products made from wood-polymer composites by the injection molding process based on micromechanical analysis. For this purpose numerical analysis was carried out for the product model with geometry of the sample intended for the uniaxial tensile test. To determine the actual fiber orientation after the manufacturing process, the orientation tensor values were calculated using Autodesk Moldflow Insight 2016 software. The micromechanical calculations were performed using Digimat FE commercial code. The results (stress-strain characteristics) of the numerical simulations taking into account the calculated fiber orientation tensor were compared to the experiment. To produce the wood-polymer composite, the polypropylene polymer matrix was Moplen HP 648T. As the filler Lignocel C120 wood fibers made by Rettenmeier & Sohns company were applied. A composite with a 10 vol.% content of wood fibers in the polymer was manufactured in the extrusion process by means of a Zamak EHP 25 extruder. For specimen manufacturing a Dr. Boy 55E injection molding machine equipped with a two cavity injection mold was used. Before the numerical simulations the uniaxial tensile test was performed using a Zwick Roell Z030 testing machine. The specimens were tested at the speed of 50 mm/min according to the PN-EN ISO 527 standard. The obtained stress-strain characteristics were used as a verification criterion for further numerical analysis. Moreover, the mechanical properties of the same composite products were predicted for hypothetical fiber orientation types. It was noted that the selection of fiber orientation has a significant impact on the quality of the obtained results compared to the experiment.

Keywords: **wood-polymer composites, numerical homogenization, micromechanical analysis, fiber orientation, injection molding process**

PROGNOZOWANIE WPŁYWU ORIENTACJI WŁÓKIEN NA WYBRANE WŁAŚCIWOŚCI WYTRZYMAŁOŚCIOWE KOMPOZYTÓW TYPU DREWNO-POLIMER

Przedstawiono ocenę wpływu orientacji włókien na właściwości wytrzymałościowe wyrobów kompozytowych na przykładzie wyrobów z kompozytu typu drewno-polimer formowanych w technologii wtryskiwania. Przeprowadzono analizę numeryczną dla modelu wyrobu o geometrii próbki przeznaczonej do próby jednoosiowego rozciągania. W celu uzyskania danych o powtryskowej orientacji włókien w matrycy polimerowej przeprowadzono analizę numeryczną procesu wtryskiwania za pomocą oprogramowania Autodesk Moldflow Insigth 2016. Uzyskano w ten sposób wartości tensora orientacji włókien dla zadanych parametrów technologicznych procesu wytwarzania wyrobu. Obliczenia mikromechaniczne (analizy właściwości struktury kompozytu) przeprowadzono z wykorzystaniem oprogramowania Digimat FE. Wyniki analizy numerycznej dla obliczonej wartości tensora orientacji włókien porównano z eksperymentem. Ponadto, w celu ułatwienia definiowania w systemach CAE właściwości kompozytu wykonano prognozowanie jego właściwości mechanicznych dla hipotetycznych, uproszczonych przypadków orientacji włókien. Potwierdzono, iż dobór orientacji napełniacza (włókien) ma znaczący wpływ na zgodność prognozowanych właściwości kompozytu z wynikami badań eksperymentalnych.

Słowa kluczowe: **kompozyty polimerowo-drzewne WPC, homogenizacja numeryczna, analiza mikromechaniczna, orientacja włókien, formowanie wtryskowe**

INTRODUCTION - BASIC THEORY OF FIBER ORIENTATION

When predicting the mechanical properties of polymer composites, it is very important to determine, in addition to other factors (e.g. filler and polymer matrix properties, phase boundary and adhesion problems etc.) the orientation of the filler in the polymer matrix.

The orientation of fibers in the polymer matrix can be written by an ellipsoidal shaped inclusion, which defines their arrangement. The general orientation of the ellipsoid is shown in Figure 1. The second order tensor (1) defines the three-dimensional orientation of

fibers in the polymer matrix [1]. Equation (1) describes the graphical presentation of the calculated values and eigenvectors of the tensor orientation.

$$a_{ij}=\begin{bmatrix} a_{11} & a_{12} & a_{13} \\ a_{21} & a_{22} & a_{23} \\ a_{31} & a_{32} & a_{33} \end{bmatrix} \rightarrow \begin{bmatrix} \lambda_1 & 0 & 0 \\ 0 & \lambda_2 & 0 \\ 0 & 0 & \lambda_3 \end{bmatrix};\begin{bmatrix} e_1 & e_2 & e_3 \end{bmatrix} \quad (1)$$

The nine tensor components are reduced to five independent components, wherein: $a_{11}+a_{22}+a_{33}=1$.

The fiber orientation defines then the three main tensor components:

- a_{11} - the fiber orientation along the flow direction (0 – 1),
- a_{22} - the fiber orientation perpendicular to the flow direction (0 – 1),
- a_{33} - the fiber orientation slope in plane 1-3 (–0.5 – 0.5),

These vectors define the location of the fibers, giving statistical proportions of eigenvalues (0 to 1) specifying their distribution with respect to the main directions. This information is used for the orientation of the ellipsoid which defines the arrangement of the fiber.

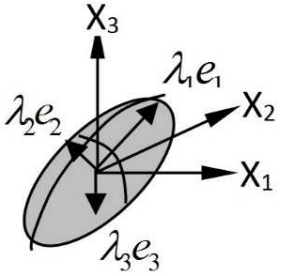

Fig. 1. General arrangement of ellipsoid defining fiber orientation
Rys. 1. Elipsoida definiująca orientację włókna

To calculate the fiber orientation in the polymer matrix the Tucker-Folgar model is often applied [2]:

$$\frac{Da_{ij}}{dt}=-\frac{1}{2}\left(\omega_{ik}a_{kj}-a_{ik}\omega_{kj}\right)+\frac{1}{2}\lambda\left(\dot{\gamma}_{ik}a_{kj}+a_{ik}\dot{\gamma}_{kj}-2a_{ijkl}\dot{\gamma}_{kl}\right)+2C_I\dot{\gamma}\left(\delta_{ij}-3a_{ij}\right) \quad (2)$$

where: a_{ji} - fiber orientation tensor, w_{ij} - vorticity tensor, γ_{ij} - strain rate tensor, C_1 - interaction coefficient of fibers.

The elastic properties of the composite are mostly calculated based on the Halpin-Tsai micromechanical model [3]:

$$\frac{P}{P_m}=\frac{1+\zeta\eta V_f}{1-\zeta V_f} \quad (3)$$

wherein:

$$\eta=\frac{\frac{P_f}{P_m}-1}{\frac{P_f}{P_m}+1} \quad (4)$$

where: P - the corresponding composite modulus, P_f, P_m - the fiber and matrix corresponding modulus, ζ - the parameter of the composite characteristics (a measure of reinforcement geometry which depends on loading conditions), V - the fiber volume fraction in the polymer matrix, f - the reference index of the fiber, m - the reference index of the matrix.

To determine the thermal expansion coefficients the Rosen-Hashin model is often used [4].

NUMERICAL HOMOGENIZATION

The mechanical properties of composites can be predicted using homogenization methods. Analytical methods are often used for this. The limitations related to using analytical homogenization methods require additional calculation methods. Therefore, in recent years numerical methods of directly calculating effective material data have become increasingly numerous and significant [5]. Most of these methods are only developed with respect to the linear strain range - the range of small deformations. Due to the growing calculating power of computers, several methods have been developed to predict the nonlinear behavior of composite materials. Numerical calculations can be performed in 2D space. This solution allows the values that appear in the cross section of the material to be calculated. However, there are some constraints resulting from the specificity of the solution to the problem (e.g. flow direction only penetrating the modeled surface, etc.) [6, 7]. In most recent years, more simulation packages have been equipped with the ability to solve 3D problems. Discretization usually consists in dividing the area into tetrahedral finite elements (FE). Such modeling is devoid of the fundamental limitations of 2D technology but is much more demanding in terms of the calculating power of a PC. One of the main types of FE used in microstructural calculations is the Voxel finite element. Each Voxel FE is assigned to the phase material where its center is located. It is intended for the discretization of a representative volume element (RVE) in cases where it is difficult to exactly reproduce the shape of the matrix and the analyzed inclusions [8].

One of the simulation packages that uses homogenization methods is Digimat software. Digimat is a nonlinear, large-scale platform for modeling materials and structures, consisting of several modules. This software includes the Digimat FE module, which uses the numerical homogenization method.

To perform the strength micromechanical analysis it is important to introduce data that describe the orientation of the inclusion (e.g. fiber). The orientation of each individual fiber is described by the unit vector p along its axis of rotation, which in turn can be determined in 3D space by means two spherical angles: theta and phi (Fig. 2) [9-12].

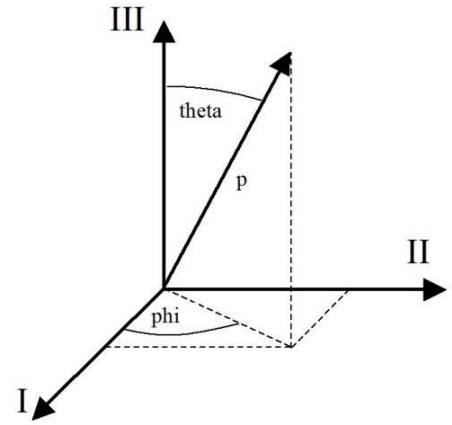

Fig. 2. Definition of orientation p vector definition based on theta and phi angles

Rys. 2. Definicja wektora orientacji p za pomocą kątów theta i Phi

To perform micromechanical calculations in Digimat FE software, there are the following possibilities to define the orientation of the inclusions [13]:

a) Fixed - all the fibers contained in the RVE are aligned in the same direction. Orientation vector p is then defined by two spherical angles: theta and phi. In the case of a composite reinforced with short fibers, the fibers often lie in the (I, II) plane. In such a case, theta should be close to 90^o while phi could be any value between 0^o and 180^o, depending on the main orientation of the fibers in the (I, II) plane.
b) Tensor - a simple but efficient way to describe an orientation distribution in the RVE. It is a simplification of what is called the orientation distribution function (ODF) - $\psi(p)$. The ODF gives the probability density to find an inclusion with orientation vector p.
c) Random 2D - the inclusions are randomly oriented in the (I,II) plane. This is a particular case of an orientation tensor for which a_{11} and a_{22} are equal to 0.5 and all the other terms are null.
d) Random 3D - the inclusions are randomly oriented in all three dimensions. This is a particular case of an orientation tensor for which all the diagonal components are equal to 1/3 and all the off-diagonal terms are null.

EXPERIMENTAL PROCEDURES AND NUMERICAL CALCULATIONS

In order to produce the wood-polymer composite, polypropylene Moplen HP 648T for the polymer matrix was used. As the filler Lignocel C120 wood fibers (WF) made by Rettenmeier & Sohns company were applied. Furthermore, Fusabond P613 as an adhesion promoter with a melt flow rate (MFR) = 49 g/10 min was added. The composite with a 10 vol.% content wood fibers in polymer was manufactured in the extrusion process by means of a Zamak EHP 25 extruder. To produce specimens a Dr. Boy 55E injection molding machine equipped with a two cavity injection mold was used. The processing parameters of the injection molding process used to manufacture the uniaxial tensile specimens are summarized in Table 1.

TABLE 1. **Adjustable parameters of injection molding process**
TABELA 1. **Parametry nastawne procesu formowania wtryskowego**

Parameter	Unit	Value
Mold temperature	[°C]	40
Melt temperature	[°C]	190
Flow rate	[cm^3/s]	20
Cooling time	[s]	35
Packing time	[s]	20
Packing pressure	[MPa]	30

Before the numerical simulations, the uniaxial tensile test was performed using a Zwick Roell Z030 testing machine. Ten specimens were tested at the speed of 50 mm/min according to the PN-EN ISO 527 standard. The obtained stress-strain characteristics were used as a verification criterion for further numerical analysis.

Then numerical simulations of the injection molding process were performed by means of Autodesk Moldflow Insight 2016 commercial code. The processing and selected strength properties of the WPC were determined based on other papers [14, 15]. The numerical model of the molded piece was discretized using approx. 100 000 tetrahedral finite elements. Analysis of the fiber orientation was performed on the basis of the flow analysis in a mold cavity taking into account the orientation of the flow vectors. The general aspect ratio of the fibers equal to 10 was adopted by means of microscopic measurement. In the calculations of the fiber orientation the following micromechanical models were used: Tucker-Folgart [2], Halpin-Tsai [3] and Rosen-Hashine [4].

The results of the flow numerical simulations (Fig. 3) showed the high value of the first order orientation tensor in the measuring area of the sample, which indicates the highest fiber orientation. As the geometry changes along the cavity geometry, the flowing polymer, passing through the measuring area of the specimen, expanded, which increased the disorientation of fibers in the grip section of the sample. In this area the lowest value of the first order orientation tensor is visible. The greatest fiber orientation disturbance in this area was because the wood fibers strike the mold cavity wall at the end of the flow. As a result of the calculations, among others, the fiber probability distribution in the polymer matrix, represented by the orientation tensor, was obtained (Fig. 3). The tensor components are interpreted as the probability of fiber arrangement in the main directions, i.e. along the flow direction, transverse to the flow direction and in the thickness of the mold cavity. The high probability of fiber orientation in a given direction is represented by

a tensor value close to 1 [1]. In the measured area of the specimen the fiber orientation tensor had the following value: a[1,1] = 0.73, a[2,2] = 0.18, a[3,3] = 0.09. These results are very important to perform micromechanical calculations to predict the stress-strain characteristics of the polymer composites [15].

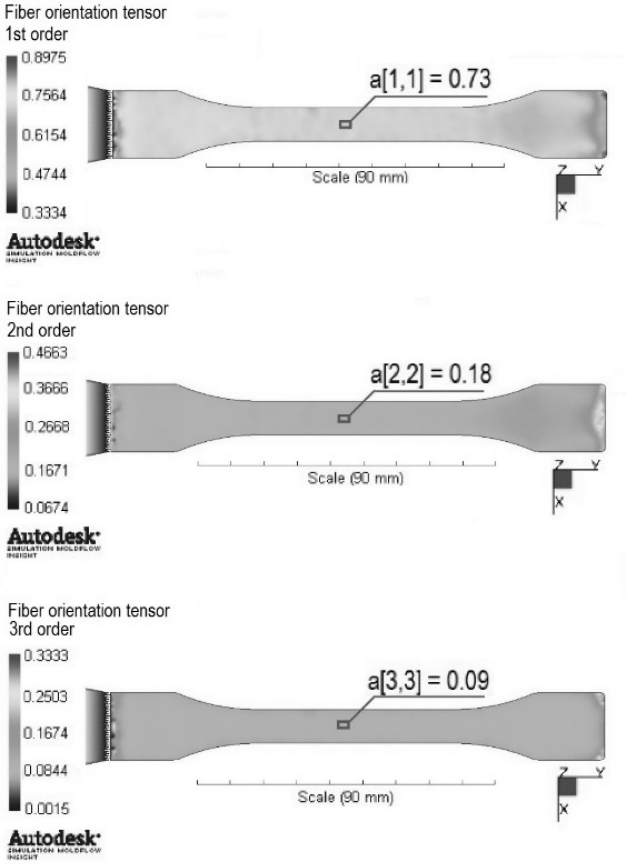

Fig. 3. Calculated values of fiber orientation tensor (1-, 2-, 3-order) in chosen area of specimen (10% WF)

Rys. 3. Obliczone wartości tensora orientacji włókien (1, 2, 3 rzędu) w określonym obszarze próbki (10% WD)

MICROMECHANICAL ANALYSIS

Then micromechanical analysis for various fiber orientations in the polymer matrix was conducted. In order to carry out advanced micromechanical analysis, the geometric data of the fibers were defined by means DIGIMAT FE software. Based on the input data, six micromechanical analyses were performed for six different types of fiber orientation:

a) real orientation - on the basis of numerical simulation,
b) theta = 90°, phi = 90°,
c) theta = 180°, phi = 90°,
d) theta = 90°, phi = 180°,
e) random 2D orientation,
f) random 3D orientation.

The curved cylinder geometry of the fibers, among others, was chosen for analysis. This type of geometry ensures good compliance of the calculated results with the experiment ones. This conclusion is confirmed based on the stress-strain characteristics results (Fig. 4) [15]. Moreover these calculated characteristics were carried out with the implemented orientation tensor value (Fig. 3) on the basis of the Autodesk Moldflow simulation results. This high compatibility with the experiment prompted the authors to perform additional micromechanical calculations for exemplary, different, fiber orientations, but uniform in the whole sample.

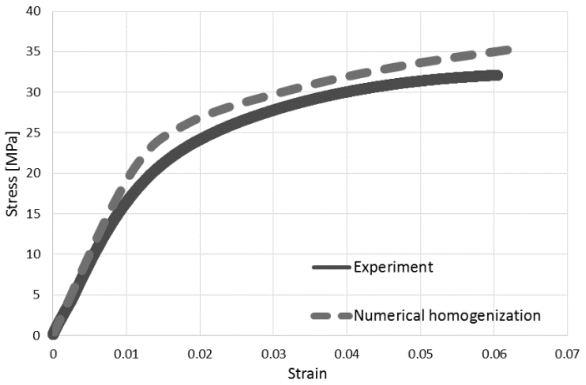

Fig. 4. Comparison of stress-strain characteristics on basis of numerical homogenization (with calculated fiber orientation tensor values) and experiment

Rys. 4. Porównanie charakterystyk naprężenie-odkształcenie otrzymanych na podstawie numerycznej homogenizacji (z obliczonymi wartościami tensora orientacji włókien) i eksperymentu

In order to carry out numerical homogenization by means of DIGIMAT FE software, the input data of the fiber orientation, geometry and percentage in RVE (Table 2) were introduced. For all the types of fiber orientation, the same RVE dimensions were defined. The RVE dimensions were large enough to determine the real distribution of fibers in the polymer matrix, but also small enough to make good calculations. The representative volume elements were digitized for each of the six analyses by means of the same number of Voxel finite elements (FE) (Table 2).

TABLE 2. **Input data for micromechanical analysis using Digimat FE**

TABELA 2. **Dane wejściowe do analizy mikromechanicznej przy użyciu Digimat FE**

Fiber diameter	0.01 mm
Fiber length	0.1 mm
Fiber length to diameter ratio (L/D)	10
Fiber volume content	0.106445
RVE dimensions	0.2x0.1x0.1 mm
Number of Voxel FE in RVE	250 000

After arrangement of the fibers in the polymer matrix the RVE was discretized using 250000 FE according to the preset orientation tensor. The visualizations of the RVE before and after discretization for the specified six types of fiber orientation are shown in Table 3.

TABLE 3. **Visualization of different cases of fiber orientation in RVE (for curved cylinder geometry of fibers): before (left) and after discretization (right)**

TABELA 3. **Wizualizacja wybranych przypadków orientacji włókien w RVE (dla przyjętej geometrii włókna typu skręcony cylinder): przed (po lewej) i po dyskretyzacji (po prawej)**

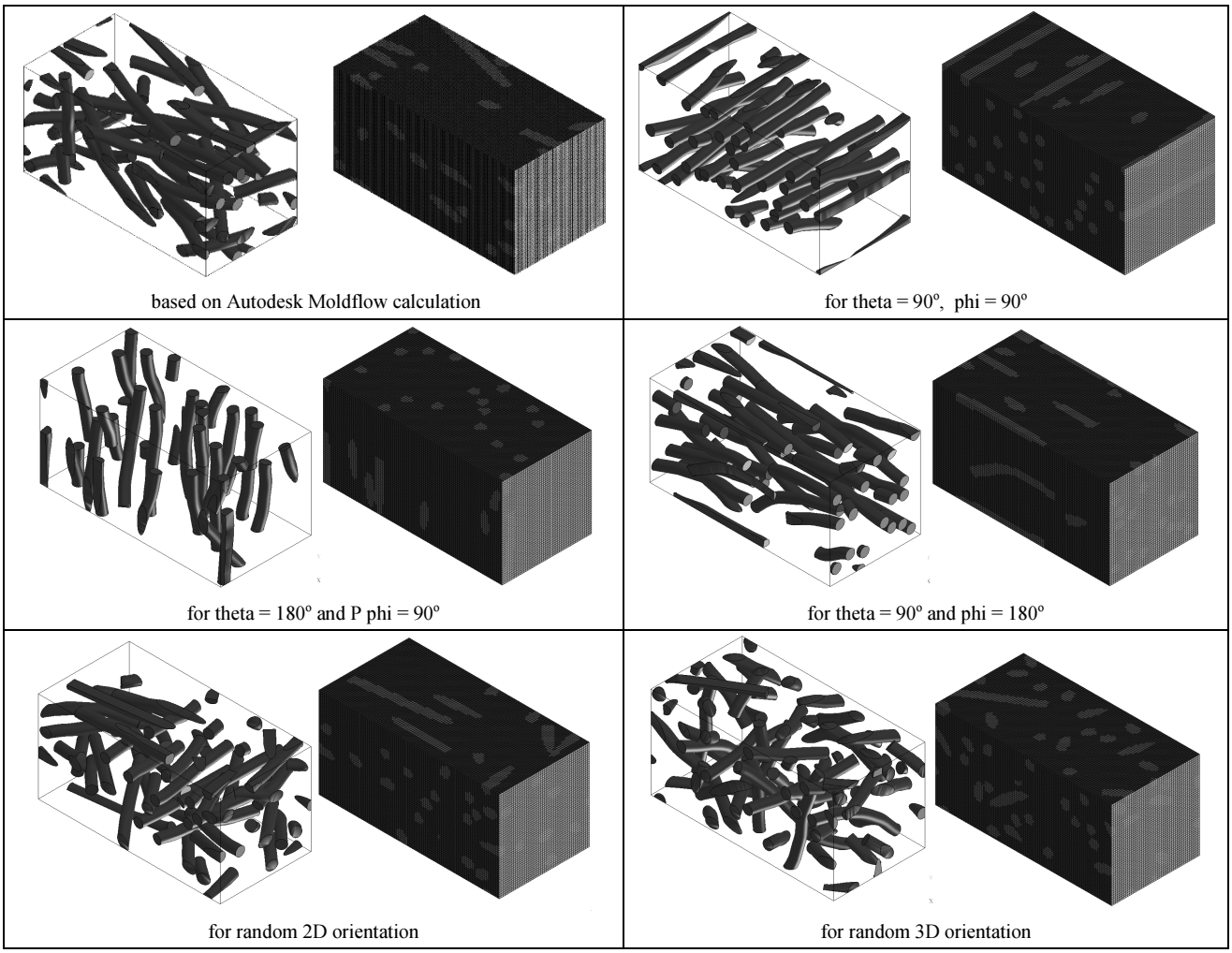

One of the main computational problems was proper distribution of the fibers in the RVE for the defined wood fiber (WF) volume content of 0.1064 = approx. 10 vol.%. The calculations were performed for the assumed cases of fiber orientation. Very high compatibility was obtained between the preset volume content and the calculated volume content for the adopted types of orientation of fibers. As we can see (Fig. 5), there are slight differences in the volume content obtained for different types of fiber orientation. The biggest difference in the obtained volume content was the RVE whose fibers were characterized by orientation of the theta angle = 180° and phi angle = 90%. The calculated value of 0.0699 volume content deviates by 34% from the input value. This is due to the perpendicular orientation of the fibers relative to the stretching direction of the samples, where the fibers are longer than the height of the RVE.

The time to generate and discretize RVE for different types of fiber orientation is interesting data (Fig. 6). The shortest time was received for the orientation with theta angle = 90° and phi angle = 180° this is due to the fact that all the fibers are unidirectional oriented and fit within the specified RVE geometry. On the other hand, the longest time was received for the Random 3D orientation of fibers. This is due to the fact that each fiber has a different orientation, hence the solver has more calculations make in order to locate the fibers in the polymer matrix.

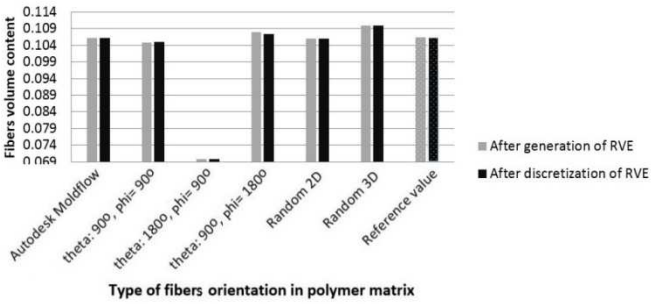

Fig. 5. Calculated volume content of fibers in analyzed RVE (for reference fiber volume content of 0.106445 set as input value)

Rys. 5. Obliczona zawartość objętościowa włókien w analizowanym RVE (dla wartości referencyjnej wynoszącej 0,106445, która została ustawiona jako wartość wejściowa)

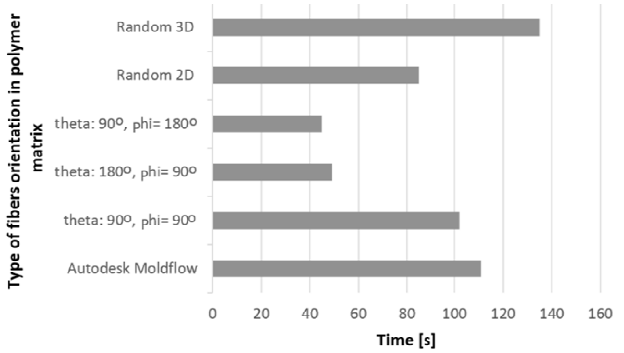

Fig. 6. Time to generate and discretize RVE for different types of fiber orientation

Rys. 6. Czas generowania i dyskretyzacji RVE dla różnych typów orientacji włókien

It is also worth analyzing the actual number of packed fibers in the RVE for the given volume share (Fig. 7). By analyzing the results, it can be seen that for most types of orientation there were 27 or 28 fibers in the RVE. In turn, the smallest number of fibers in the RVE was for theta angle = 180º and phi angle = 90º and it was 19.

One of the most important results is the stiffness matrix (Fig. 8). In the case of the stiffness matrix using a numerical model of homogenization, the matrix was filled in all the cells, indicating a slight numerical error.

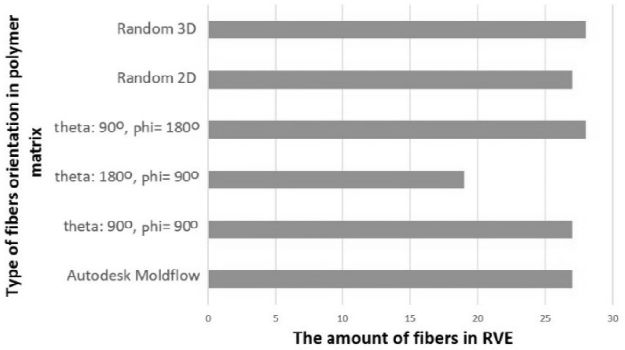

Fig. 7. Generated number of fibers in RVE for prescribed fiber content of 0.106445

Rys. 7. Wygenerowana liczba włókien w RVE dla zadanego udziału wynoszącego 0,106445

a)

	11	22	33	12	23	13
11	3788.59	2350.88	2315.22	-12.1463	-9.75874	23.7813
22	2350.88	3624.89	2281.07	7.3617	-0.0361329	-4.63391
33	2315.22	2281.07	3624.67	0.574974	7.86392	1.61387
12	-12.1463	7.36171	0.574978	649.093	-11.4478	-8.87849
23	-9.75874	-0.036134	7.86392	-11.4478	650.194	1.97659
13	23.7813	-4.6339	1.61388	-8.87849	1.97659	622.652

b)

	11	22	33	12	23	13
11	3610.17	2278.3	2258.66	0.0021396	-0.0039939	-0.608111
22	2278.3	4064.58	2290.1	0.0171475	-0.055099	-0.982372
33	2258.66	2290.1	3618.12	0.00155673	-0.0107647	0.533724
12	0.0021396	0.0171475	0.00155673	576.007	-2.26163E-005	-0.00314799
23	-0.0039939	-0.055099	-0.0107647	-2.26163E-005	576.007	0.00130151
13	-0.608112	-0.982372	0.533723	-0.00314799	0.00130151	668.467

c)

	11	22	33	12	23	13
11	3467.38	2182.57	2194.91	-0.144704	0.00224101	0.000250854
22	2182.57	3460.6	2199.9	-0.115847	0.000859236	-0.000215664
33	2194.91	2199.9	3732.22	-0.181172	0.0142516	0.00635583
12	-0.144704	-0.115847	-0.181172	636.257	-0.000874236	0.001496
23	0.00224102	0.000859251	0.0142516	-0.000874236	575.85	1.96511E-006
13	0.000250857	-0.000215666	0.00635582	0.001496	1.96517E-006	575.85

d)

	11	22	33	12	23	13
11	3988.44	2285.69	2295.12	0.00958623	-1.09392	0.0548343
22	2285.69	3634.11	2265.63	0.00112897	-5.08792	0.00373015
33	2295.13	2265.63	3631.26	0.00219338	-2.29591	0.00932187
12	0.00958625	0.00112898	0.00219339	576.018	0.00291336	-3.85289E-005
23	-1.09392	-5.08793	-2.29591	0.00291336	672.509	0.00209515
13	0.0548343	0.00373014	0.00932185	-3.85289E-005	0.00209515	576.018

e)

	11	22	33	12	23	13
11	3778.66	2397.76	2290.76	-3.4312	6.85002	-2.40118
22	2434.72	3712.46	2328.68	1.43284	-6.50157	3.51784
33	2415.25	2385.27	3615.47	15.5908	25.8373	-9.34887
12	-14.457	-5.53509	9.02825	660.824	4.92814	-9.14752
23	0.0481858	0.21984	-0.0532863	-0.145767	615.693	13.3689
13	-0.999752	-0.378736	-0.865888	0.0300085	13.3577	627.463

f)

	11	22	33	12	23	13
11	3648.53	2351.4	2331.06	-14.31	-25.0082	8.59662
22	2351.4	3683.18	2354.5	-5.75861	-27.8677	10.8625
33	2331.06	2354.5	3641.51	8.96132	7.11967	-2.72242
12	-14.31	-5.7586	8.96133	661.056	5.44131	-9.64203
23	-25.0082	-27.8677	7.11968	5.44131	662.539	13.4137
13	8.59661	10.8624	-2.72243	-9.64202	13.4137	658.114

Fig. 8. Stiffness matrices for WPC (10% WF) for different fiber orientations: a) on basis of simulation using Autodesk Modflow Insight software, b) for theta angle = 90º, phi angle = 90º, c) for theta angle = 180º, phi angle = 90º, d) for theta angle = 90º, phi angle = 180º, e) for Random 2D type, f) for Random 3D type

Rys. 8. Macierze sztywności dla WPC (10% WD) dla orientacji włókien: a) na podstawie symulacji w programie Autodesk Modflow Insight, b) dla kątów Teta = 90º, Fi = 90º, c) dla kątów Teta = 180º, Fi = 90º, d) dla kątów Teta = 90º, Fi = 180º, e) dla orientacji losowej typu 2D, f) dla orientacji losowej typu 3D

TABLE 4. **Calculated properties of WPC (in elastic range) for various types of wood fiber orientations**

TABELA 4. **Prognozowane właściwości kompozytów (w zakresie sprężystym) dla różnych przypadków orientacji włókien drzewnych**

	Type of fiber orientation					
	Based on flow simulation	**Theta angle = 90º, phi angle = 90º**	**Theta angle = 180º, phi angle = 90º**	**Theta angle = 90º, phi angle = 180º**	**Random 2D type**	**Random 3D type**
Density [kg/m^3]	1006	1006	1006	1006	1006	1006
Young's modulus E1 [MPa]	1994.0	1924.8	1811.5	2209.6	1890.0	1825.68
Young's modulus E2 [MPa]	1857.9	2287.7	1800.9	1933.3	1829.5	1829.5
Young's modulus E3 [MPa]	1940.1	1920.4	2021.9	1921.9	1815.44	1815.4
Poisson's ratio v12	0.4199	0.3245	0.4107	0.3845	0.4073	0.3901
Poisson's ratio v21	0.3913	0.3857	0.4084	0.3364	0.3909	0.3909
Poisson's ratio v13	0.3702	0.4188	0.3459	0.3922	0.3713	0.3880
Poisson's ratio v31	0.3598	0.4179	0.3861	0.3411	0.3858	0.3858
Poisson's ratio v23	0.3757	0.3922	0.3492	0.4113	0.3964	0.3964
Poisson's ratio v32	0.3924	0.3292	0.3221	0.4089	0.3933	0.3933
Shear modulus G12 [MPa]	661.7	576.0	636.3	576.0	660.7	660.6
Shear modulus G23 [MPa]	665.7	672.5	575.9	672.5	615.4	661.6
Shear modulus G13 [MPa]	618.9	576.0	575.9	576.0	627.2	657.6

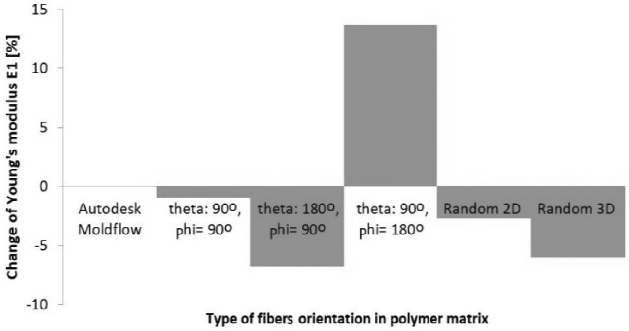

Fig. 9. Change of Young's modulus in E1 direction (relative to calculated value using Autodesk Moldflow software verified by experiment)

Rys. 9. Zmiana modułu Younga w kierunku E1 (względem wartości obliczonej za pomocą programu Autodesk Moldflow, zweryfikowanej eksperymentalnie)

CONCLUSIONS

1. The methods of numerical homogenizations allow good compatibility to be obtained between the results of approximately experimental research and numerical analyses. Proper selection of the fiber orientation has a significant impact on the correctness of the obtained results. This is due to the fact that the examined area of the composite is analyzed on the micromechanical level, very sensitive to small changes in input parameters and calculating conditions.
2. The influence of the adopted fiber orientation model in the calculations is very important because it also determines the effective volume content of fibers in the RVE. The worst compatibility was obtained for the orientation with theta angle = 180^o and phi angle = 90^o (the percentage error was about 34%). For the other types of orientation, very high compatibility of the obtained fiber content with the set value was found. Furthermore, it was noted that for the RVE, after generation and discretization, slightly different results were obtained in the volume content of the fibers.
3. The choice of fiber orientation affects the number of fibers in the RVE. It can be seen that for most types of orientation there were 27 or 28 fibers in the RVE. The smallest number of fibers in the RVE for fiber orientation with theta angle =180^o and phi angle = 90^o was 19.
4. The discretization and RVE generation times are interesting data. For unidirectional oriented fibers these times were the shortest. This is due to the fact that for all the fibers the same orientation tensor value was used. On the other hand, the longest discretization and RVE generation times were noticed for the Random 3D orientation of fibers. In this case the computational solver had to perform the calculation for each individual fiber, which increased the calculation time.
5. The most consistent result for numerical homogenization is associated with the choice of fiber orientation with the direct orientation tensor value. The very large changes in the Young's modulus values (from about −7% to about 14% - relative to the calculated orientation using Autodesk Moldflow software, verified by experiment) for different fiber orientations indicate the importance of fiber orientation in micromechanical calculations. This reflects the real, non-standard problems to determine the orientation of the wood fiber in the polymer matrix
6. The use of simplifications in the material models of polymer composites during strength analyses of the products allows to omit expensive and time-consuming analyses of plastic flow in the mold cavities (taking into account the effect of fiber orientation) to be omitted only if an appropriate model of fiber orientation is chosen. Simplifications in fiber orientation modeling help to reduce computational problems due to, among others, simplification of the stiffness matrix and reduction of the calculation time. This is particularly important in the strength analysis of large-sized products.

REFERENCES

[1] Advani S.G., Tucker III C.L., The use of tensors to describe and predict fiber orientation in short fiber composites, Journal of Rheology 1987, 31, 8, 751-784.

[2] Tucker III C.L., Liang E., Stiffness prediction for unidirectional short-fiber composites: Review and evaluation, Composites Science and Technology 1999, 59, 5, 655-671.

[3] Halpin J.C., Kardos J.L., The Halpin-Tsai equations: A review, Polymer Engineering & Science 1976, 16(5), 345-352.

[4] Rosen B.W., Hashin Z., Effective thermal expansion coefficients and specific heats of composite materials, International Journal of Engineering Science 1970, 8, 2, 157-161.

[5] Bendsøe M.P., Kikuchi N., Generating optimal topologies in structural design using a homogenization method, Computer Methods in Applied Mechanics and Engineering 1988, 71, 2, 197-224.

[6] Abdulle A., Numerical homogenization methods, 2013, 1-18 (No. EPFL-ARTICLE-184958).

[7] Bouchart V., Brieu M., Kondo D., Abdelaziz M.N., Macroscopic behavior of a reinforced elastomer: micromechanical modelling and validation, Mechanics & Industry 2007, 8, 3, 199-205.

[8] Doghri I., Tinel L., Micromechanics of inelastic composites with misaligned inclusions: numerical treatment of orientation, Computer Methods in Applied Mechanics and Engineering 2006, 195, 13, 1387-1406.

[9] Hine P.J., Duckett R.A., Davidson N., Clarke A.R., Modelling of the elastic properties of fibre reinforced composites. I: Orientation measurement, Composites Science and Technology 1993, 47, 1, 65-73.

[10] Chin W.K., Liu H.T., Lee Y.D., Effects of fiber length and orientation distribution on the elastic modulus of short fiber reinforced thermoplastics, Polymer Composites 1988, 9, 1, 27-35.

[11] Gupta M., Wang K.K., Fiber orientation and mechanical properties of short fiber reinforced injection molded composites: Simulated and experimental results, Polymer Composites 1993, 14, 5, 367-382.

[12] Zhu Y.T., Blumenthal W.R., Lowe T.C., Determination of non-symmetric 3-D fiber-orientation distribution and average fiber length in short-fiber composites, Journal of Composite Materials 1993, 31, 13, 1287-1301.

[13] DIGIMAT software documentation, e-Xstream engineering, 2016.

[14] Frącz W., Janowski G., Strength analysis of molded pieces produced from wood-polymer composites (WPC) including their complex structures, Composites Theory and Practice 2016, 16, 4, 260-265.

[15] Frącz W., Janowski G., Influence of homogenization methods in prediction of strength properties for WPC composites, Applied Computer Science 2017, 13, 3, 77-89.

